Proceedings of IDETC/CIE 2005
ASME 2005 International Design Engineering Technical Conferences
& Computers and Information in Engineering Conference
September 24-28, 2005, Long Beach, California USA

DETC2005-85104

COMPARISON OF THREE-DIMENSIONAL FLEXIBLE BEAM ELEMENTS FOR DYNAMIC ANALYSIS: FINITE ELEMENT METHOD AND ABSOLUTE NODAL COORDINATE FORMULATION

A. L. Schwab
Laboratory for Engineering Mechanics
Delft University of Technology
Mekelweg 2, NL-2628 CD Delft, The Netherlands
Phone: +31-15-2782701, Fax: +31-15-2782150
Email: a.l.schwab@wbmt.tudelft.nl

J. P. Meijaard
School of MMME
The University of Nottingham
University Park, Nottingham NG7 2RD
United Kingdom

ABSTRACT

Three formulations for a flexible spatial beam element for dynamic analysis are compared: a finite element method (FEM) formulation, an absolute nodal coordinate (ANC) formulation with a continuum mechanics approach and an ANC formulation with an elastic line concept where the shear locking of the asymmetric bending mode is suppressed by the application of the Hellinger–Reissner principle. The comparison is made by means of an eigenfrequency analysis on two stylized problems. It is shown that the ANC continuum approach yields too large torsional and flexural rigidity and that shear locking suppresses the asymmetric bending mode. The presented ANC formulation with the elastic line concept resolves most of these problems.

1 Introduction

Several finite element method (FEM) formulations for spatial finite beam elements to be used in multibody system dynamics programs can be found in the literature. A common approach is to use a small displacement formulation with respect to a reference frame that describes the overall rigid body motion of the beam [1, 2]. In order to reduce the number of degrees of freedom, a limited number of assumed modes for the deformations are chosen. The linear contribution to the stiffness matrix due to pre-stresses can be included by adding a geometric stiffness matrix [3].

A different way to describe the motion of the elements is by using nodal coordinates that describe the configuration of the element with respect to an inertial reference frame. This approach is more in line with traditional non-linear finite element formulations used in statics. A convenient element formulation was given by Van der Werff and Jonker [4], which was implemented in the program SPACAR [5] and extended further in Meijaard [6]. A number of generalized deformations are defined that are invariant under rigid body motions, so arbitrary rigid body motions can be described. On the other hand, the so-called absolute nodal coordinate (ANC) formulation was recently proposed by Shabana [7]. This formulation describes the position of a material point within the element by interpolations based on the Cartesian absolute coordinates of the nodal points and on gradients of these positions with respect to a reference configuration. This leads to constant mass matrices for the elements, at the cost of a more complicated description for the stiffness.

The purpose of the present paper is to make a comparison between the finite element formulation for a two-noded spatial beam as described in [6] and a corresponding absolute nodal coordinate formulation as given in [8, 9]. It will be shown that the continuum mechanics formulation given by [9] has some fundamental shortcomings. It is not possible to describe the warping of the cross-section, so the shear stiffness lacks a shear correction factor and the torsional rigidity is too large for non-circular cross-sections of the beam. Furthermore, the anticlastic deformation of the cross-section cannot be described, so the resulting flexural rigidity is too large, and the shear deformation and bending deformation are coupled for antisymmetric bending, so effectively the beam has only a single bending mode. A modification of the absolute modal coordinate formulation that is described in [8], with a stiffness description based on the elastic line concept, is also included in the comparison. The modifications consist of the inclusion of in-plane deformations of the cross-section, so the linearized stiffness matrix has the appropriate rank, and the elimination of the coupling between bending and shearing for the antisymmetric bending mode by means of a Hellinger–Reissner [10] formulation. In order to limit the efforts in the comparison and to show the main differences in the formulation clearly, only linearized eigenfrequencies for a single beam are compared.

The organization of the paper is as follows. After this introduction, the FEM formulation and subsequently the ANC formulation and the proposed modifications are described. Then results on the eigenfrequencies of two stylized problems are presented and discussed. The paper ends with some conclusions.

2 FEM Beam

The finite beam element is a Timoshenko beam based on the elastic line concept. This means essentially that the beam is slender and the cross-section is doubly symmetric and more or less solid. The presentation of the element mainly follows [6].

The configuration of the element (Fig. 1) is determined by the position and orientation of the two end nodes, by which it can be coupled to and interact with other elements. The positions of the end nodes p and q are given by their coordinates $\mathbf{x}^p$ and $\mathbf{x}^q$ in a global inertial system $Oxyz$, whereas the orientations are determined by orthogonal triads of unit vectors $(\mathbf{e}_x^p, \mathbf{e}_y^p, \mathbf{e}_z^p)$ and $(\mathbf{e}_x^q, \mathbf{e}_y^q, \mathbf{e}_z^q)$ which are rigidly attached to the nodes.

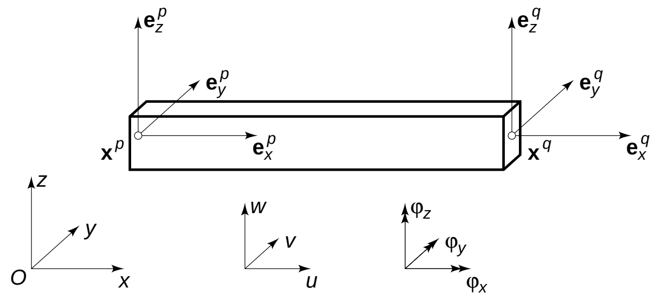

Figure 1. FEM beam.

The unit vector $\mathbf{e}_x$ is perpendicular to the average warped cross-sectional plane of the beam in the sense of Cowper [11], and $\mathbf{e}_y$ and $\mathbf{e}_z$ are in the principal directions of the cross-section. In the absence of shear deformations, $\mathbf{e}_x$ is tangent to the elastic line of the beam. The change in orientation of the triads at the end nodes is determined by an orthogonal rotation matrix. This matrix can be parametrized by a choice of parameters, denoted by $\boldsymbol{\vartheta}$, such as, Euler angles, modified Euler angles, Rodrigues parameters and Euler parameters. In the SPACAR [5] software system we use Euler parameters, but this choice is immaterial to the description of the properties of the element.

2.1 Elastic Forces

The elastic forces are derived with the elastic line concept. To prevent shear locking, the shear deformation will be directly tied to the bending. Such a modification of the bending stiffness can already be found in the book by Przemieniecki [12].

The element has 6 degrees of freedom as a rigid body, while the nodes have 12 degrees of freedom. Hence the deformation that is determined by the end nodes of the element can be described by 6 independent generalized strains, which are functions of the positions and orientations of the nodes and the initially undeformed geometry. With $\mathbf{l} = \mathbf{x}^q - \mathbf{x}^p$ and l the length of the undeformed beam, we define the 6 generalized strains as

$$
\begin{array}{lll}
\varepsilon_1 = \sqrt{\mathbf{l}^T\mathbf{l}} - l, & & \text{(elongation)} \\
\varepsilon_2 = l(\mathbf{e}_z^{pT}\mathbf{e}_y^q - \mathbf{e}_y^{pT}\mathbf{e}_z^q)/2, & & \text{(torsion)} \\
\varepsilon_3 = -\mathbf{l}^T\mathbf{e}_z^p, & \varepsilon_4 = \mathbf{l}^T\mathbf{e}_z^q, & \text{(bending in xz-plane)} \\
\varepsilon_5 = \mathbf{l}^T\mathbf{e}_y^p, & \varepsilon_6 = -\mathbf{l}^T\mathbf{e}_y^q. & \text{(bending in xy-plane)}
\end{array}
\tag{1}
$$

These generalized strains, which may be compared to what Argyris called natural modes [13], are invariant under arbitrary rigid body motions, so they truly measure the amount of strain in the element. If we group the positions and orientations of the nodes in a vector $\mathbf{x} = (\mathbf{x}^p, \boldsymbol{\vartheta}^p, \mathbf{x}^q, \boldsymbol{\vartheta}^q)$ and denote the vector of generalized deformations by $\boldsymbol{\varepsilon}$, then we can write for the generalized strains (1) symbolically

$$
\varepsilon_i = D_i(x_k), \qquad i = 1, \ldots, 6,\ k = 1, \ldots, 12. \tag{2}
$$

The dual quantities of the generalized strains $\boldsymbol{\varepsilon}$ are the generalized stresses $\boldsymbol{\sigma}$. The physical meaning of these stresses is found by equating the internal virtual work of the elastic forces $\boldsymbol{\sigma}^T\delta\boldsymbol{\varepsilon}$ to the external virtual work $\mathbf{f}^T\delta\mathbf{u}$ of the nodal forces. Substitution of the virtual generalized strains derived from (2) results in

$$
\sigma_i\delta\varepsilon_i = \sigma_i D_{i,k}\delta u_k = f_k\delta u_k \quad \forall \quad \delta u_k, \tag{3}
$$

with the small nodal displacements and rotations $\mathbf{u}^T = (\mathbf{u}^{pT}, \boldsymbol{\vartheta}^{pT}, \mathbf{u}^{qT}, \boldsymbol{\vartheta}^{qT})$, and a subscript after the comma to denote partial derivatives. From this we derive the force equilibrium conditions for the element as

$$f_k = D_{i,k}\sigma_i, \tag{4}$$

In the case of small deformations, the generalized stresses have a clear physical meaning. As the deformed and undeformed geometry are nearly the same, we consider the undeformed situation in which the beam central axis coincides with the global x-axis. For the rotational parameters $\boldsymbol{\vartheta}$ we choose the small rotations about the three coordinate axes φ_x, φ_y and φ_z. The Jacobian of the generalized strains then takes the values

$$D^0_{i,k} = \begin{pmatrix} -1 & 0 & 0 & 0 & 0 & 0 & 1 & 0 & 0 & 0 & 0 & 0 \\ 0 & 0 & 0 & -l & 0 & 0 & 0 & 0 & 0 & l & 0 & 0 \\ 0 & 0 & 1 & 0 & -l & 0 & 0 & 0 & -1 & 0 & 0 & 0 \\ 0 & 0 & -1 & 0 & 0 & 0 & 0 & 0 & 1 & 0 & l & 0 \\ 0 & -1 & 0 & 0 & 0 & -l & 0 & 1 & 0 & 0 & 0 & 0 \\ 0 & 1 & 0 & 0 & 0 & 0 & 0 & -1 & 0 & 0 & 0 & l \end{pmatrix} \tag{5}$$

The equilibrium nodal force system according to (4) is then given by

$$\begin{aligned} \mathbf{F}^p &= (-\sigma_1, \sigma_6 - \sigma_5, \sigma_3 - \sigma_4), \ \mathbf{M}^p = (-\sigma_2 l, -\sigma_3 l, -\sigma_5 l), \\ \mathbf{F}^q &= (\sigma_1, \sigma_5 - \sigma_6, \sigma_4 - \sigma_3), \quad \mathbf{M}^q = (\sigma_2 l, \sigma_4 l, \sigma_6 l). \end{aligned} \tag{6}$$

From this result we interpret that σ_1 is the normal force, $\sigma_2 l$ is the torsion moment, and $\sigma_3 l, \sigma_4 l, \sigma_5 l$ and $\sigma_6 l$ are the bending moments at the nodes p and q.

If for each beam element the strains remain small by dividing the overall beam in sufficiently many elements, then the usual linear stress-strain relation can be applied which results for the generalized stresses and strains in

$$\sigma_i = S_{ij}\varepsilon_j \qquad i, j = 1, \ldots, 6, \tag{7}$$

where the stiffness $S_{ij} = \mathrm{diag}(S_1, S_2, \mathbf{S}_3, \mathbf{S}_4)$ is given by

$$\begin{aligned} S_1 &= EA/l, & S_2 &= S_t/l^3, \\ \mathbf{S}_3 &= \frac{EI_y}{(1+\Phi_z)l^3}\begin{pmatrix} 4+\Phi_z & -2+\Phi_z \\ \text{symm.} & 4+\Phi_z \end{pmatrix}, & \Phi_z &= \frac{12EI_y}{GAk_z l^2} \\ \mathbf{S}_4 &= \frac{EI_z}{(1+\Phi_y)l^3}\begin{pmatrix} 4+\Phi_y & -2+\Phi_y \\ \text{symm.} & 4+\Phi_y \end{pmatrix}, & \Phi_y &= \frac{12EI_z}{GAk_y l^2}. \end{aligned} \tag{8}$$

Here, E is the modulus of elasticity (Young's modulus), G is the shear modulus, A is the area of the cross-section, S_t is the torsional stiffness, I_y and I_z are the area moments of inertia of the cross-section with respect to the principal axes, and k_y and k_z are the shear coefficients according to Cowper [11]. Note that the inclusion of the shear deformation is done by a slightly modified stiffness matrix [12]. This tying of the shear deformation to the bending by means of the statics of the beam prevents problems of shear locking.

Finally the element stiffness matrix is obtained by taking partial derivatives of the nodal forces $\mathbf{f}$ with respect to the small nodal displacements $\mathbf{u}$, resulting in a tangent stiffness matrix

$$\bar{K}_{ij} = D_{k,i}S_{kl}D_{l,j} + D_{k,ij}\sigma_j, \tag{9}$$

which consists of two parts. The last part is the geometric stiffness matrix, which, evaluated in the undeformed and unstressed geometry, is identical to zero, and the first part is the linear stiffness matrix

$$K^0_{ij} = D^0_{k,i}S_{kl}D^0_{l,j}. \tag{10}$$

2.2 Inertia Forces

The derivation of the consistent mass formulation for the flexible spatial beam element is based on the elastic line concept. To arrive at a Timoshenko beam the rotary inertia of the cross-section will be included by a separate interpolation of the orientation of the cross-section along the elastic line.

The interpolation for the positions on the elastic line for finite deformation is taken as

$$\begin{aligned} \mathbf{r}(\xi) = &(1 - 3\xi^2 + 2\xi^3)\mathbf{x}^p + (\xi - 2\xi^2 + \xi^3)l\mathbf{e}^p_x \\ &+ (3\xi^2 - 2\xi^3)\mathbf{x}^q + (-\xi^2 + \xi^3)l\mathbf{e}^q_x, \end{aligned} \tag{11}$$

where $\xi = x/l$. The first part of the mass matrix is obtained by evaluating the integral

$$m\int_0^1 \delta\dot{\mathbf{r}}^T\ddot{\mathbf{r}}d\xi, \tag{12}$$

where m is the total mass of the beam. If the rotations at the nodes are parametrized by $\boldsymbol{\vartheta}^p$ and $\boldsymbol{\vartheta}^q$, this results in a mass matrix

$$\mathbf{M} = \frac{m}{420}\begin{pmatrix} 156\mathbf{I} & 22l\mathbf{A} & 54\mathbf{I} & -13l\mathbf{B} \\ & 4l^2\mathbf{A}^T\mathbf{A} & 13l\mathbf{A}^T & -3l^2\mathbf{A}^T\mathbf{B} \\ & & 156\mathbf{I} & -22l\mathbf{B} \\ \text{symm.} & & & 4l^2\mathbf{B}^T\mathbf{B} \end{pmatrix} \tag{13}$$

and inertia terms which are quadratic in the velocities [6], where

$$\mathbf{A} = \partial\mathbf{e}^p_x/\partial\boldsymbol{\vartheta}^p, \qquad \mathbf{B} = \partial\mathbf{e}^q_x/\partial\boldsymbol{\vartheta}^q. \tag{14}$$

Clearly the mass matrix is not constant and moreover, the equations of motion contain convective inertia forces. The second part of the mass matrix takes into account the rotary inertia of the cross-section. The rotations of the cross-section along the elastic line are interpolated in the same manner as the elastic line but with the inclusion of the shear deformation resulting in

$$
\begin{aligned}
\varphi_x &= (1-\xi)\varphi_x^p + \xi\varphi_x^q \\
\varphi_y &= \frac{1}{1+\Phi_z}\{[6\xi(1-\xi)](w^p - w^q)/l \\
&\quad +[(1-4\xi+3\xi^2)+(1-\xi)\Phi_z]\varphi_y^p \\
&\quad +[(-2\xi+3\xi^2)+\xi\Phi_z]\varphi_y^q)\}, \\
\varphi_z &= \frac{1}{1+\Phi_y}\{[6\xi(1-\xi)](v^q - v^p)/l \\
&\quad +[(1-4\xi+3\xi^2)+(1-\xi)\Phi_y]\varphi_z^p \\
&\quad +[(-2\xi+3\xi^2)+\xi\Phi_y]\varphi_z^q)\},
\end{aligned}
\tag{15}
$$

where the small nodal displacements and rotations are given by

$$
\mathbf{u} = (u^p, v^p, w^p, \varphi_x^p, \varphi_y^p, \varphi_z^p, u^q, v^q, w^q, \varphi_x^q, \varphi_y^q, \varphi_z^q) \tag{16}
$$

If we denote the mass moment of inertia along the principal axes of an infinitesimal small section by $\mathrm{d}I_x, \mathrm{d}I_y$ and $\mathrm{d}I_z$ then the following integral

$$
\int_{s=0}^{s=l} (\delta\dot{\varphi}_x \mathrm{d}I_x \ddot{\varphi}_x + \delta\dot{\varphi}_y \mathrm{d}I_y \ddot{\varphi}_y + \delta\dot{\varphi}_z \mathrm{d}I_z \ddot{\varphi}_z), \tag{17}
$$

results in a mass matrix with the contributions of the rotary inertia of the cross-section. If the principal dimension of the cross-section is h, then this contribution is of the order $(h/l)^2$ compared with the entries of the regular mass matrix (13).

3 ANC beam

In this section a two node spatial beam element according to the absolute nodal coordinate formulation will be presented. Here we follow mainly the description by Shabana and Yakoub [8, 9].

A distinguishing point in the ANC formulation is the usage of slope vectors to describe the orientation of the cross-section in the nodes, where the slope vectors are not necessarily unit vectors. This leaves more room for the cross-section to deform and change shape. It is expected [8,9] that this type of description, together with a three-dimensional continuum mechanics approach, leads to more accurate results. A well-known major advantage of this description is that it leads to a constant mass matrix. Unfortunately, the expressions for the elastic forces are more complex.

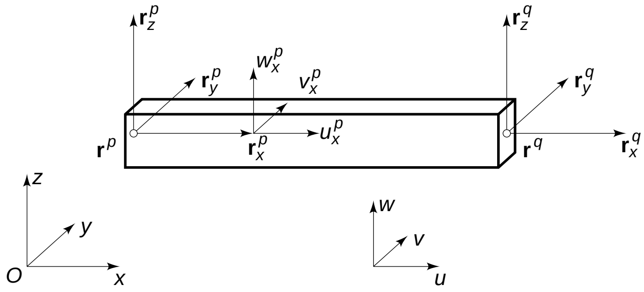

Figure 2. ANC beam

The configuration of the beam element (Fig. 2) is determined by the position and orientation of the two end nodes p and q. Each node is defined by one vector for the position $\mathbf{r}$ and three vectors for the slopes $\mathbf{r}_x, \mathbf{r}_y$ and $\mathbf{r}_z$, where every vector is expressed in a global inertial system $Oxyz$. Thus the element has 24 nodal coordinates given by the vector

$$
e = [\mathbf{r}^{pT}, \mathbf{r}_x^{pT}, \mathbf{r}_y^{pT}, \mathbf{r}_z^{pT}, \mathbf{r}^{qT}, \mathbf{r}_x^{qT}, \mathbf{r}_y^{qT}, \mathbf{r}_z^{qT}]^T \tag{18}
$$

The location of an arbitrary point $\mathbf{r}$ in the beam is determined by the interpolation

$$
\mathbf{r} = \mathbf{S}(x, y, z)\mathbf{e} \tag{19}
$$

where $\mathbf{S}$ is the element shape function and $\mathbf{e}$ is the vector of nodal coordinates. The shape function is obtained using polynomials which are in this case cubic in x and linear in y and z, where the x-direction is initially along the central axis of the beam. The element shape function matrix $\mathbf{S}$ is now defined as

$$
\mathbf{S} = [S_1\mathbf{I}, S_2\mathbf{I}, S_3\mathbf{I}, S_4\mathbf{I}, S_5\mathbf{I}, S_6\mathbf{I}, S_7\mathbf{I}, S_8\mathbf{I}], \tag{20}
$$

where $\mathbf{I}$ is the 3 by 3 identity matrix and the polynomials

$$
\begin{aligned}
&S_1 = 1 - 3\xi^2 + 2\xi^3, && S_2 = l(\xi - 2\xi^2 + \xi^3), \\
&S_3 = l(1-\xi)\eta, && S_4 = l(1-\xi)\zeta, \\
&S_5 = 3\xi^2 - 2\xi^3, && S_6 = l(-\xi^2 + \xi^3), \\
&S_7 = l\xi\eta, && S_8 = l\xi\zeta,
\end{aligned}
\tag{21}
$$

with the non-dimensional coordinates

$$
\xi = x/l, \quad \eta = y/l, \quad \zeta = z/l, \tag{22}
$$

and l the initial length of the beam. The initial undeformed configuration where the beam central axis coincides with the global

x-axis is

$$\mathbf{r}^0 = \mathbf{S}\mathbf{e}^0 \tag{23}$$

with the initial nodal coordinates $\mathbf{e}^0$ as

$$\mathbf{e}^0 = [\mathbf{0}^T, \mathbf{e}_x^T, \mathbf{e}_y^T, \mathbf{e}_z^T, l\mathbf{e}_x^T, \mathbf{e}_x^T, \mathbf{e}_y^T, \mathbf{e}_z^T]^T \tag{24}$$

with fixed triads $(\mathbf{e}_x, \mathbf{e}_y, \mathbf{e}_z)$ of the global inertial system $Oxyz$. Indeed, substitution of $\mathbf{e}^0$ in (23) leads to the identities $\mathbf{r}^0 = (x, y, z)^T$.

3.1 Elastic Forces, continuum approach

The elastic forces are derived from a general continuum mechanics approach. We start from the displacements $\mathbf{u}$ of an arbitrary point of the beam expressed in the global $Oxyz$ coordinate system as given by

$$\mathbf{u} = \mathbf{r} - \mathbf{r}_0. \tag{25}$$

Substitution of these displacements in the Green–Lagrange strain tensor

$$\varepsilon_{ij} = \frac{1}{2}(u_{i,j} + u_{j,i} + u_{k,i}u_{k,j}), \qquad i,j,k = x,\dots,z. \tag{26}$$

where partial derivatives are denoted by $u_{x,y} = \partial u_x/\partial y \dots$, leads to the strain tensor expressed in the absolute coordinates $\mathbf{r}$ and their derivatives as

$$\varepsilon_{ij} = \frac{1}{2}(r_{k,i}r_{k,j} - \delta_{ij}) = \frac{1}{2}\begin{pmatrix} \mathbf{r}_{,x}^T\mathbf{r}_{,x} - 1 & \mathbf{r}_{,x}^T\mathbf{r}_{,y} & \mathbf{r}_{,x}^T\mathbf{r}_{,z} \\ & \mathbf{r}_{,y}^T\mathbf{r}_{,y} - 1 & \mathbf{r}_{,y}^T\mathbf{r}_{,z} \\ \text{symm.} & & \mathbf{r}_{,z}^T\mathbf{r}_{,z} - 1 \end{pmatrix} \tag{27}$$

From this we identify 6 independent strain components which we write in the form of a strain vector ε such that the vector dot product $\frac{1}{2}\boldsymbol{\sigma}^T\boldsymbol{\varepsilon}$ represents the elastic energy. This strain vector is now

$$\begin{aligned} &\varepsilon_1 = \tfrac{1}{2}\left(\mathbf{r}_{,x}^T\mathbf{r}_{,x} - 1\right), \ \varepsilon_2 = \tfrac{1}{2}\left(\mathbf{r}_{,y}^T\mathbf{r}_{,y} - 1\right), \ \varepsilon_3 = \tfrac{1}{2}\left(\mathbf{r}_{,z}^T\mathbf{r}_{,z} - 1\right), \\ &\varepsilon_4 = \mathbf{r}_{,x}^T\mathbf{r}_{,y}, \qquad \varepsilon_5 = \mathbf{r}_{,y}^T\mathbf{r}_{,z}, \qquad \varepsilon_6 = \mathbf{r}_{,z}^T\mathbf{r}_{,x} \end{aligned} \tag{28}$$

The virtual work of the elastic forces now can be written as

$$\delta W = \int_V \boldsymbol{\sigma}^T \delta\boldsymbol{\varepsilon} \mathrm{d}V. \tag{29}$$

Under the assumption of a linear elastic isotropic material the stress vector $\boldsymbol{\sigma}$ is related to the strain vector as

$$\boldsymbol{\sigma} = \mathbf{E}\boldsymbol{\varepsilon}, \tag{30}$$

where the non-zero elastic coefficients $\mathbf{E}$ are given by

$$\begin{aligned} &E_{ij} = \frac{2G}{(1-2\nu)}\begin{pmatrix} 1-\nu & \nu & \nu \\ \nu & 1-\nu & \nu \\ \nu & \nu & 1-\nu \end{pmatrix}, \ i,j = 1,\dots,3, \\ &E_{kk} = G, \qquad\qquad\qquad\qquad k = 4,\dots,6. \end{aligned} \tag{31}$$

Equating the virtual work of the elastic forces with the virtual work of the external nodal forces $\mathbf{Q}$ as in

$$\int_V \boldsymbol{\sigma}^T \delta\boldsymbol{\varepsilon} \mathrm{d}V = \mathbf{Q}^T\delta\mathbf{e}, \tag{32}$$

yields the elastic nodal forces expressed in terms of the nodal displacements

$$\mathbf{Q} = \int_V (\partial\boldsymbol{\varepsilon}/\partial\mathbf{e})^T \mathbf{E}\boldsymbol{\varepsilon} \mathrm{d}V \tag{33}$$

The tangent stiffness matrix is obtained by linearizing the elastic forces with respect to the nodal displacements

$$\bar{\mathbf{K}} = \int_V (\partial\boldsymbol{\varepsilon}/\partial\mathbf{e})^T\mathbf{E}(\partial\boldsymbol{\varepsilon}/\partial\mathbf{e})\mathrm{d}V + \int_V (\partial^2\boldsymbol{\varepsilon}/\partial\mathbf{e}^2)^T\mathbf{E}\boldsymbol{\varepsilon}\ \mathrm{d}V \tag{34}$$

The last matrix is the geometric stiffness matrix, which evaluated in the undeformed and unstressed geometry is identical to zero, whereas the first matrix is the linear stiffness matrix

$$\mathbf{K} = \int_V (\partial\boldsymbol{\varepsilon}/\partial\mathbf{e})^T\mathbf{E}(\partial\boldsymbol{\varepsilon}/\partial\mathbf{e})\mathrm{d}V. \tag{35}$$

Finally, we will evaluate the linear stiffness matrix in the undeformed geometry. With the notion that the slopes in the initially undeformed geometry are identical to the global directions

$$(\partial\mathbf{r}_{,x}/\partial\mathbf{e})^0 = \mathbf{e}_x, \qquad (\partial\mathbf{r}_{,y}/\partial\mathbf{e})^0 = \mathbf{e}_y, \qquad (\partial\mathbf{r}_{,z}/\partial\mathbf{e})^0 = \mathbf{e}_z \tag{36}$$

the partial derivatives of the strain vector evaluated at this initial undeformed configuration become

$$(\partial\boldsymbol{\varepsilon}/\partial\mathbf{e})^0 = \begin{pmatrix} \mathbf{S}_{1,x} \\ \mathbf{S}_{2,y} \\ \mathbf{S}_{3,z} \\ \mathbf{S}_{1,y} + \mathbf{S}_{2,x} \\ \mathbf{S}_{2,z} + \mathbf{S}_{3,y} \\ \mathbf{S}_{3,x} + \mathbf{S}_{1,z} \end{pmatrix}^0 \tag{37}$$

Substitution into (35) and evaluating the integral over the volume of the beam leads to the desired linear stiffness matrix

$$\mathbf{K}^0 = \int_V (\partial\boldsymbol{\varepsilon}/\partial\mathbf{e})^{0T}\mathbf{E}(\partial\boldsymbol{\varepsilon}/\partial\mathbf{e})^0 \mathrm{d}V. \tag{38}$$

3.2 Inertia forces

The absolute nodal coordinate formulation leads to inertia forces which can be expressed as the product of a constant mass matrix times the accelerations of the nodal coordinates. There are no inertia forces which are quadratic in the velocities. The constant mass matrix is defined as

$$\mathbf{M} = \int_V \rho\mathbf{S}^T\mathbf{S}\mathrm{d}V. \tag{39}$$

The above integral defines a mass matrix which only depends on the mass distribution and the dimensions of the beam and, under the assumption of a consistent shape function, captures all linear and rotary inertia effects.

3.3 Elastic forces, elastic line approach

As an alternative to the general continuum approach [9] where we suspect the forces to show shear locking, we propose to derive the elastic forces for the beam from an elastic line concept. For the interpolation of points of the beam we will still use the same cubic/linear form as in the continuum approach (19, 20) but all deformations, extension, shear, torsion, and bending, will be evaluated on the elastic line.

First we define the slopes on the elastic line as

$$\mathbf{r}_x = \mathbf{r}_{,x}(x,0,0), \qquad \mathbf{r}_y = \mathbf{r}_{,y}(x,0,0), \qquad \mathbf{r}_z = \mathbf{r}_{,z}(x,0,0). \tag{40}$$

With these slopes we define 9 generalized deformations

$$\begin{array}{lll} \varepsilon_x = \frac{1}{2}(\mathbf{r}_x^T\mathbf{r}_x - 1), & \varepsilon_y = \frac{1}{2}(\mathbf{r}_y^T\mathbf{r}_y - 1), & \varepsilon_z = \frac{1}{2}(\mathbf{r}_z^T\mathbf{r}_z - 1), \\ \gamma_{yz} = \mathbf{r}_y^T\mathbf{r}_z & \gamma_{xy} = \mathbf{r}_x^T\mathbf{r}_y, & \gamma_{xz} = \mathbf{r}_x^T\mathbf{r}_z, \\ \kappa_x = \frac{1}{2}(\mathbf{r}_z^T\mathbf{r}_y' - \mathbf{r}_y^T\mathbf{r}_z'), & \kappa_y = \mathbf{r}_z^T\mathbf{r}_x', & \kappa_z = -\mathbf{r}_y^T\mathbf{r}_x' \end{array} \tag{41}$$

where a prime denotes a derivative with respect to x. The first four, $\varepsilon_x, \varepsilon_y, \varepsilon_z$ and γ_{yz} represent the extension of the beam and the deformation of the cross-section, γ_{xy} and γ_{xz} are the transverse shear deformations, κ_x is the torsion, and κ_y and κ_z are the bending deformations.

The strain energy W^e of the beam is the sum of the strain energies of the extension and deformation of the cross-section

$$W_l = \frac{1}{2}l\int_0^1 (A\bar{\varepsilon}_i E_{ij}\bar{\varepsilon}_j)\mathrm{d}\xi, \qquad i,j = 1,\ldots,4, \tag{42}$$

with the strains $\bar{\varepsilon}_i = (\varepsilon_x, \varepsilon_y, \varepsilon_z, \gamma_{yz})$ and the elasticity coefficients E_{ij} as in (31), the transverse shear deformation

$$W_s = \frac{1}{2}l\int_0^1 (GAk_y\gamma_{xy}^2 + GAk_z\gamma_{xz}^2)\mathrm{d}\xi \tag{43}$$

and the torsion and bending

$$W_t = \frac{1}{2}l\int_0^1 (S_t\kappa_x^2)\mathrm{d}\xi, \quad W_b = \frac{1}{2}l\int_0^1 (EI_y\kappa_y^2 + EI_z\kappa_z^2)\mathrm{d}\xi, \tag{44}$$

making $W^e = W_l + W_s + W_t + W_b$. With the cubic/linear interpolation on the elastic line according to (20) and (40) we suspect that adding the contribution of the shear deformation according to (43) will result in shear locking. Therefore we propose to add the shear stiffness by means of the Hellinger–Reissner principle [10]. In this approach we are free to define both the displacements field and the stress distribution. This can be very advantageous if the stress distribution, usually from an engineering point of view, is known beforehand. In the case of pure shear deformation we assume that the shear forces will vary linearly over the elastic line of the element. The strain energy of the shear deformation is the sum of the shear in the y and the z direction. We start with shear forces in the z direction, and assume a linear shear stress distribution according to,

$$\tau_{xz} = \mathbf{N}\boldsymbol{\tau}^*, \tag{45}$$

with the shape function

$$\mathbf{N} = ((1-\xi), \xi), \tag{46}$$

and the nodal shear stresses

$$\boldsymbol{\tau}^* = (\tau_{xz}^p, \tau_{xz}^q)^T. \tag{47}$$

The strain energy according to he Hellinger–Reissner principle is

$$W_{sz}^* = \int_V (\tau_{xz}^T\gamma_{xz} - W_c(\tau_{xz}))\mathrm{d}V, \tag{48}$$

where W_c is the complementary shear stress energy according to

$$W_c(\tau_{xz}) = \frac{1}{2Gk_z}\tau_{xz}^T\tau_{xz}, \tag{49}$$

with shear factor k_z to account for the fact that the shear stress is not uniformly distributed over the cross-section [11]. Substitution of the linear shear stress distribution from (45) results in a strain energy

$$W_{sz}^* = \int_V (\boldsymbol{\tau}^{*T} \mathbf{N}^T \gamma_{xz} - \frac{1}{2Gk_z} \boldsymbol{\tau}^{*T} \mathbf{N}^T \mathbf{N} \boldsymbol{\tau}^*) \mathrm{d}V, \tag{50}$$

with the shear strain distribution γ_{xz} according to (41). For this shear strain energy we seek a stationary value with respect to the generalized shear stress parameters $\boldsymbol{\tau}^*$, resulting in

$$\delta W_{sz}^* = \int_V \delta\boldsymbol{\tau}^{*T} (\mathbf{N}^T \gamma_{xz} - \frac{1}{Gk_z} \mathbf{N}^T \mathbf{N} \boldsymbol{\tau}^*) \mathrm{d}V = 0. \tag{51}$$

Integration over the volume yields

$$\mathbf{W}_{xz} - \mathbf{F}_z \boldsymbol{\tau}^* = 0 \tag{52}$$

with the energy terms

$$\mathbf{W}_{xz}(\mathbf{e}) = Al \int_0^1 (\mathbf{N}^T \gamma_{xz}(\mathbf{e})) \mathrm{d}\xi \tag{53}$$

which are in general non-linear functions in the nodal coordinates $\mathbf{e}$ and the constant coefficient matrix

$$\mathbf{F}_z = \frac{Al}{Gk_z} \begin{pmatrix} 1/3 & 1/6 \\ 1/6 & 1/3 \end{pmatrix} \tag{54}$$

From this we can solve for the generalized shear stress parameters

$$\boldsymbol{\tau}^* = \mathbf{S}_z \mathbf{W}_{xz}, \qquad \mathbf{S}_z = \mathbf{F}_z^{-1} = \frac{Gk_z}{Al} \begin{pmatrix} 4 & -2 \\ -2 & 4 \end{pmatrix}. \tag{55}$$

Substitution in the original shear energy function yields the shear energy according to the Hellinger–Reissner principle

$$W_{sz}^* = \frac{1}{2} \mathbf{W}_{xz}^T \mathbf{S}_z \mathbf{W}_{xz}. \tag{56}$$

The shear strain energy for shear forces in the y directions, W_{sy}^* can be derived in the same manner resulting in a total shear strain energy function of

$$W_s^* = \frac{1}{2} \mathbf{W}_{xy}^T \mathbf{S}_y \mathbf{W}_{xy} + \frac{1}{2} \mathbf{W}_{xz}^T \mathbf{S}_z \mathbf{W}_{xz}. \tag{57}$$

The strain energy for the beam with the adapted shear stiffness according to the Hellinger–Reissner principle now becomes

$$W^{e*} = W_l + W_s^* + W_t + W_b. \tag{58}$$

The linear stiffness matrix is found in the same manner as in Section 3.1. The elastic forces are determined from equating the variation of the elastic energy with the virtual work of the nodal forces

$$\delta W^{e*} = (\partial W^{e*} / \partial \mathbf{e}) \delta \mathbf{e} = \mathbf{Q}^{eT} \delta \mathbf{e} \tag{59}$$

Then the linear stiffness matrix is found by linearizing the elastic forces with respect to the nodal coordinates at the undeformed reference configuration

$$\mathbf{K} = (\partial \mathbf{Q}^e / \partial \mathbf{e})^0. \tag{60}$$

Because the elastic energy is a direct sum of contributions due to extension, shear, torsion, and bending the same holds for the stiffness matrix. The individual contributions to the stiffness matrix are, for the extension

$$\mathbf{K}_l = l \int_0^1 (A(\bar{\varepsilon}_{i,\mathbf{e}})^{0T} E_{ij} (\bar{\varepsilon}_{j,\mathbf{e}})^0) \mathrm{d}\xi, \qquad i,j = 1,\ldots,4, \tag{61}$$

for the shear deformation

$$\mathbf{K}_s = (\mathbf{W}_{xy,\mathbf{e}})^{0T} \mathbf{S}_y (\mathbf{W}_{xy,\mathbf{e}})^0 + (\mathbf{W}_{xz,\mathbf{e}})^{0T} \mathbf{S}_z (\mathbf{W}_{xz,\mathbf{e}})^0, \tag{62}$$

for the torsion

$$\mathbf{K}_t = l \int_0^1 (S_t (\kappa_{x,\mathbf{e}})^{0T} (\kappa_{x,\mathbf{e}})^0) \mathrm{d}\xi, \tag{63}$$

and for the bending

$$\mathbf{K}_b = l \int_0^1 (EI_y (\kappa_{y,\mathbf{e}})^{0T} (\kappa_{y,\mathbf{e}})^0) \mathrm{d}\xi + l \int_0^1 (EI_z (\kappa_{z,\mathbf{e}})^{0T} (\kappa_{z,\mathbf{e}})^0) \mathrm{d}\xi. \tag{64}$$

The partial derivatives of the generalized strains with respect to the nodal coordinates in the initially undeformed configuration take on even simpler forms as in (36) and (37) since the only variable is now the elastic line coordinate x.

4 Results and Discussion

In this section the three different element formulations will be compared. Since every element uses a different set of nodal coordinates, the comparison will be made by means of an eigenfrequency analysis of the free vibration of a simply supported beam and of a cantilever beam, both modelled by one element. The beam has an undeformed length l and a uniform square cross-section of width and height $h = 0.02l$. The Poisson ratio of the material is $\nu = 0.3$. The shear factors for a square cross-section are $k_y = k_z = 10(1+\nu)/(12+11\nu)$ [11]. The torsional stiffness is given by $S_t = Gk_xI_p$, with $G = E/[2(1+\nu)]$, the shear distribution factor $k_x = 0.8436$ [14], and the polar area moment of inertia $I_p = I_y + I_z$.

The first case is a simply supported beam. The boundary conditions for the FEM beam are straightforward. Both nodes are supported in the yz-plane plus the horizontal displacement in node p and the rotation along the central axis are restricted. This leaves 6 degrees of freedom, namely

$$\mathbf{u}^c = (\varphi_y^p, \varphi_z^p, u^q, \varphi_x^q, \varphi_y^q, \varphi_z^p). \tag{65}$$

For the ANC formulated element we apply the same boundary conditions, where the rotation along the central axis in node p is suppressed by fixing the displacement of the slope $\mathbf{r}_z^p$ in the y-direction, v_z^p. The remaining degrees of freedom, 18 in total, are

$$\begin{aligned}\mathbf{u}^c = (&u_x^p, v_x^p, w_x^p, u_y^p, v_y^p, w_y^p, u_z^p, w_z^p,\\ &u^q, u_x^q, v_x^q, w_x^q, u_y^q, v_y^q, w_y^q, u_z^q, v_z^q, w_z^q),\end{aligned} \tag{66}$$

where we the displacements of a slope vector $\mathbf{r}_x^p$ are denoted by (u_x^p, v_x^p, w_x^p) and so forth. The results of this analysis are presented in Table 1. The first observation that we make is that the ANC formulation yields 12 further eigenfrequencies, of which 10 are local modes with a high frequency. The first bending mode in the continuum ANC is too high by a factor $\sqrt{(1-\nu)/(1+\nu)/(1-2\nu)} \approx 1.16$, because the anticlastic deformation of the cross-section cannot be described by the continuum displacement field. Note that this result is also present in the dynamic response of the mid-point deflection of the pendulum beam from Fig. 8 in [9]. The torsional eigenfrequency is also too high, because the factor k_x is not included. The continuum ANC gives a large value for the second bending mode, because this mode is coupled to a shearing deformation, a phenomenon that is referred to as shear locking. The modified ANC formulation gives a far more realistic value. The exact values of the factors for an Euler–Bernoulli beam are π^2 and $4\pi^2$. The ANC gives good approximations for the longitudinal eigenfrequencies, because the interpolation is cubic instead of linear. Compare the numerical factors with the exact factors that follow from a slender rod theory, $(2k-1)\pi/2$, $k = 1, 2, 3, \ldots$.

Mode	FEM	ANC con.	ANC el.	unit
2 bending (symm.)	10.953	12.699	10.954	$\sqrt{\frac{EI}{ml^3}}$
2 bending (asymm.)	50.134	696.14	50.200	$\sqrt{\frac{EI}{ml^3}}$
torsion	1.5908	1.7319	1.5908	$\sqrt{\frac{GA}{ml}}$
longitudinal 1^{st}	1.6408	1.5724	1.5724	$\sqrt{\frac{EA}{ml}}$
longitudinal 2^{nd}	–	5.0546	5.0548	$\sqrt{\frac{EA}{ml}}$
longitudinal 3^{rd}	–	11.585	11.586	$\sqrt{\frac{EA}{ml}}$
	–	107.42	198.03	$\sqrt{\frac{EA}{ml}}$
10 modes	–	…	…	
	–	240.24	480.40	$\sqrt{\frac{EA}{ml}}$

Table 1. Eigenfrequencies for a simply supported beam.

The second case is a cantilever beam. The boundary conditions for the FEM beam are straightforward. The p node is fully suppressed in both displacement and orientation and the q is free. This leaves 6 degrees of freedom, namely

$$\mathbf{u}^c = (u^q, v^q, w^q, \varphi_x^q, \varphi_y^q, \varphi_z^p). \tag{67}$$

For the ANC element we first suppress the displacements of the p node. Then to suppress the rotation of the cross-section at p we suppress the displacement of the slope $\mathbf{r}_y^p$ in the x and z direction, u_y^p and w_y^p, and the slope $\mathbf{r}_z^p$ in the x direction, u_z^p. The remaining degrees of freedom, 18 in total, are

$$\begin{aligned}\mathbf{u}^c = (&u_x^p, v_x^p, w_x^p, v_y^p, v_z^p, w_z^p,\\ &u^q, v^q, w^q, u_x^q, v_x^q, w_x^q, u_y^q, v_y^q, w_y^q, u_z^q, v_z^q, w_z^q).\end{aligned} \tag{68}$$

The results of this analysis are presented in Table 2. For this case, the results for the longitudinal and torsion eigenfrequencies are as in the simple supported case. For bending, we see the same kind of phenomena as before, especially the shear locking in the second bending mode for the continuum ANC. The elastic line ANC still gives rather high values for the bending eigenvalues. This can be attributed to the difficulty in prescribing the condition of zero rotation of the cross-section for the clamped end. Because the Hellinger–Reissner formulation relaxes the rigidity against shear deformation, shear can still occur at the ends of the beam for asymmetric bending; the shear is only small in an average sense. The acurate numerical factors for the bending modes of an Euler–Bernoulli beam are 3.5156 and 22.0336.

Mode	FEM	ANC con.	ANC el.	unit
2 bending 1st	3.5316	5.1860	4.4654	$\sqrt{\frac{EI}{ml^3}}$
2 bending 2nd	34.760	361.69	59.655	$\sqrt{\frac{EI}{ml^3}}$
2 bending/shearing	–	980.38	791.50	$\sqrt{\frac{EI}{ml^3}}$
torsion	1.5908	1.7319	1.5908	$\sqrt{\frac{GA}{ml}}$
longitudinal	1.6408	1.5724	1.5724	$\sqrt{\frac{EA}{ml}}$
longitudinal 2nd	–	5.0546	5.0548	$\sqrt{\frac{EA}{ml}}$
longitudinal 3rd	–	11.585	11.586	$\sqrt{\frac{EA}{ml}}$
	–	107.43	198.06	$\sqrt{\frac{EA}{ml}}$
8 modes	–	$\cdots$	$\cdots$	
	–	240.24	480.40	$\sqrt{\frac{EA}{ml}}$

Table 2. Eigenfrequencies for a cantilever beam.

5 Conclusion

In this paper some formulations for a flexible spatial beam have been compared. In general, the FEM formulation gives good results for the linearized case. Some shortcomings in the spatial beam formulation given by [9] were found, especially that it yielded too large torsional and flexural rigidities and that shear locking effectively suppressed the asymmetric bending mode. An elastic line ANC formulation, along similar lines as in [8] has been proposed. This formulation yielded better torsional and flexural rigidities. The shear locking of the asymmetric bending mode could be suppressed by the aid of the application of the Hellinger–Reissner principle; the problem of the proper imposition of clamped boundary conditions remains.

As a direction of future research, it is desirable to develop the spatial beam ANC formulation based on the elastic line concept further.

REFERENCES

[1] Fraeijs de Veubeke, B., ‘The dynamics of flexible bodies’, *International Journal of Engineering Science* **14**, 1976, pp.895–913.

[2] Shabana, A. A., and Wehage, R. A., ‘Variable degree-of-freedom component mode analysis of inertia variant flexible mechanical systems’, *ASME Journal of Mechanisms, Transmissions, and Automation in Design* **105**, 1983, pp.371–378.

[3] Wallrapp, O., and Schwertassek, R., ‘Representation of geometric stiffening in multibody system simulation’, *International Journal for Numerical Methods in Engineering* **32**, 1991, pp.1833–1850.

[4] Werff, K. van der, and Jonker, J. B., ‘Dynamics of flexible mechanisms’, in *Computer aided analysis and optimization of mechanical system dynamics*, Haug, E. J. (ed.), Springer-Verlag, Berlin, 1984, pp.381–400.

[5] Jonker, J. B., and Meijaard, J. P., ‘SPACAR–Computer program for dynamic analysis of flexible spatial mechanisms and manipulators’, in *Multibody Systems Handbook*, Schiehlen, W. O. (ed.), Springer-Verlag, Berlin, 1990, pp. 123–143.

[6] Meijaard, J. P., ‘Validation of flexible beam elements in dynamics programs’, *Nonlinear Dynamics* **9**, 1996, pp. 21–36.

[7] Shabana, A. A., ‘Flexible multibody dynamics: review of past and recent developments’, *Multibody System Dynamics* **1**, 1997, pp.189–222.

[8] Shabana, A. A., and Yakoub, R. A., ‘Three Dimensional absolute nodal coordinate formulation for beam elements: theory’, *ASME Journal of Mechanical Design* **123**, 2001, pp. 606–613.

[9] Yakoub, R. A., and Shabana, A. A., ‘Three Dimensional absolute nodal coordinate formulation for beam elements: implementation and applications’, *ASME Journal of Mechanical Design* **123**, 2001, pp. 614–621.

[10] Reissner, E., ‘On a variational theorem for finite elastic deformations’, *Journal of Mathematics and Physics* **32**, 1953, pp. 129–135.

[11] Cowper, G. R., ‘The shear coefficient in Timoshenko’s beam theory’, *ASME Journal of Applied Mechanics* **33**, 1966, pp.335–340.

[12] Przemieniecki, J. S.,*Theory of Matrix Structural Analysis*, McGraw–Hill, New York, 1968.

[13] Argyris, J. H., ‘Continua and discontunia, an aperçu of recent developments of the matrix displacement methods’, in *Matrix Methods in Structural Mechanics*, J. S. Przemieniecki, et al. (eds.), Wright-Patterson Air Force Base, Dayton, Ohio, 1966, pp. 11–189.

[14] Timoshenko, S. P., and Goodier, J. N., *Theory of Elasticity*, McGraw–Hill, New York, 1987.